Analyses of the bearing behaviour of dowel-type fasteners by means of non-contact full-field optical deformation measurements

J.C.M. (Dennis) Schoenmakers[1], S. Svensson[2]
[1]: PhD-researcher, Eindhoven University of Technology, Eindhoven, the Netherlands
[2]: Associate professor, Denmark Technical University, Lyngby, Denmark

Abstract

Comparison of literature shows that the definition of embedding strength, i.e. the stress level at a certain deformation level, is inconsistent. Besides, the test configuration applied appears to be different, i.e. specimens supported over the entire length or only supported at the ends (full-constrained or unconstrained specimens). In literature several attempts have been made to test perpendicular to grain splitting strength of dowel-type connections in beams, with one single fastener as well as multiple fastener connections. Based on the theory of plasticity it can be expected that single fastener connections will fail by ongoing bearing of the fasteners, and not by primary splitting of the main beam.

This paper reveals additional knowledge into the bearing behaviour of single fastener connections. By means of non-contact full field deformation measurements it is shown that the strains in the bearing zone look somewhat different when comparing full-constrained or unconstrained specimens. In addition, the unconstrained specimens behave similar as the beam specimens which is not surprisingly since both test configurations induce bending stresses.

Calculations show that, although the strain shape underneath the fasteners deviates among the tested configurations, i.e. triangular or circular, all tests can be explained by the theory of plasticity and therefore it is concluded that stresses will be distributed through the specimens towards a larger bearing surface. Analyses of the test results shows that, as can be derived from other tests as well, the European Yield Model to provide incorrect predictions of the strength because the embedding strength currently given by Eurocode 5 [1] is incorrect. Therefore the embedding strength equations should be replaced.

1 Introduction

Timber in compression perpendicular to the grain shows hardening after an initial linear-elastic response, see Figure 1. This behaviour is a result of restrained dilatation perpendicular to the grain associated with a multi-axial stress state, and therefore the load-carrying capacity appears to be dependant of the deformation of the compressed timber fibres and the ability of load sharing through the specimen.

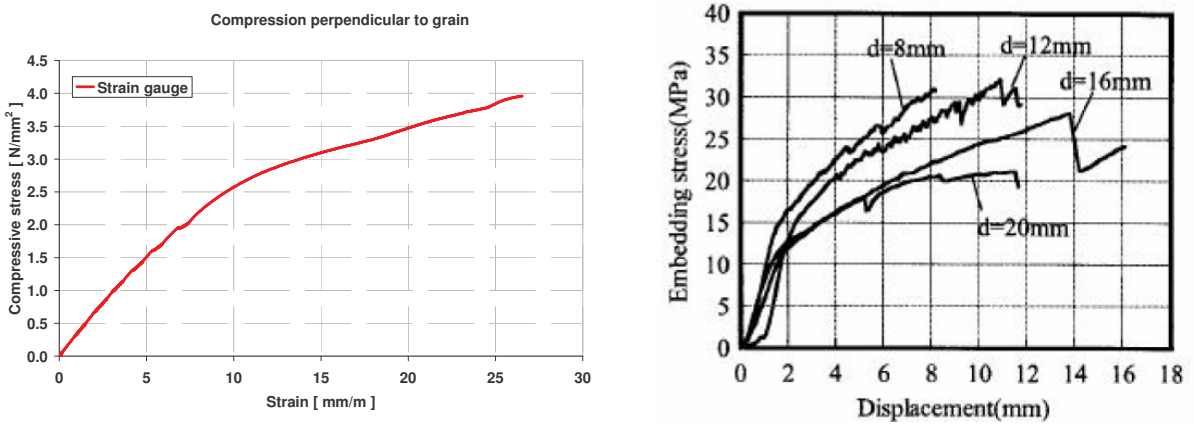

Figure 1: Load-deformation response perpendicular to the grain.
Left (sill), Right (dowel-type fastener) (From: Sawata and Yasumura [2])

Comprehensive studies of the bearing (embedding) strength of dowel-type fasteners have been reported by e.g. Leijten et al [3], Whale and Smith [4] and Sawata and Yasumura [2]. Both parallel and perpendicular to grain bearing were considered. Analyses of these test results have lead to empirical descriptions of the strength, in which timber density and fastener diameter are considered to be of significant influence. Usually, the embedding strength is regarded as the stress level beneath the fastener corresponding to a certain embedding deformation. However, due to the hardening behaviour the embedding strength perpendicular to the grain is ambiguous. According to standard EN 383 [5] the embedding strength is defined as the maximum stress level reached within 5 mm displacement. A large amount of available data in literature, Whale and Smith [4], defined embedding strength perpendicular to grain at 2.1 mm, as a result of some preliminary tests. Besides, the specimen dimensions and loading configuration vary as well. According to EN 383 [5] the specimen should be full constrained (supported over the length), while the tests by Whale and Smith [4] were conducted by means of unconstrained specimens (i.e. bending, the specimen only supported at the ends).

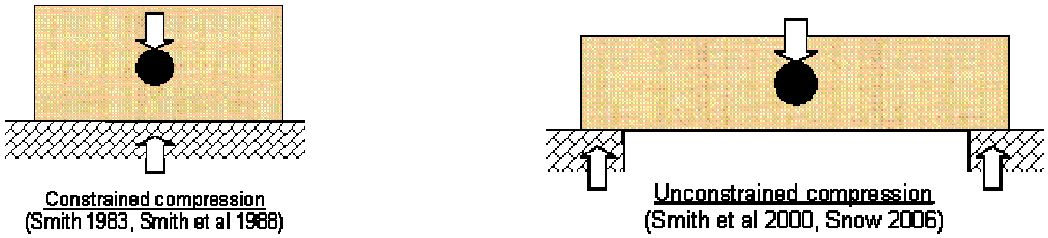

Figure 2: Constrained and unconstrained specimens to test embedding strength

It is described by Van der Put and Leijten [6] that the strength of connections loading the timber perpendicular to the grain can be estimated based on the theory of plasticity with the method of characteristics. It therefore is stated that forces underneath the dowel will be distributed through the specimens towards a larger surface. Based on compression tests on timber sills this angle is assumed to be 1:1.5 (≈34°).

The theory described in Van der Put and Leijten [6] can be extended with which the deformation level of the timber underneath the fastener as well as the timber density can be taken into account, for softwood species (yet unpublished) One of the objectives of the STSM was to obtain more insights in the angle of load spreading. Therefore ARAMIS (GOM) appeared to be a suitable measuring device.

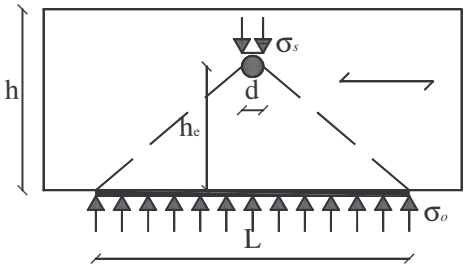

Figure 3: Loads are spread under an angle towards a larger supporting surface

Connections with one fastener loading a timber beam perpendicular to the grain are often regarded as splitting tests, i.e. splitting cracks are the primary cause of failure. As so, test results are analysed from this point of view, see Ballerini [7]. It can be shown that these tests are in fact embedding tests, and their failure has nothing to do with a primary splitting failure mechanism. Fracture in such tests appears to be a post-fracture mechanism at lower energy release rates, caused by ongoing bearing of the fastener through the timber. The second objective of this STSM was to reveal whether an embedding test and the situation described with beams behave comparable in the connection zone, i.e. angle of stress distribution.

It is well known that multiple fastener connections with a large amount of fasteners (e.g. n=10) will fail due to unstable crack propagation in grain direction. This will occur at rather low loading levels of the fasteners, i.e. the embedment stresses underneath the fasteners remain low. Splitting seems to be more or less a material parameter independent of the number of fasteners. To the contrary a connection with only one or two fasteners will fail as a result of ongoing bearing of the fasteners in the timber, i.e. the timber underneath the fasteners will fail in compression perpendicular to the grain. The fastener is highly loaded in this case.

If the bearing behaviour and strength of one single fastener in the connection zone can be described more accurately, it should be possible to describe whether a connection will fail due to splitting or due to bearing (embedment) for the prevailing boundary conditions. The figure shows a sketch of this statement.

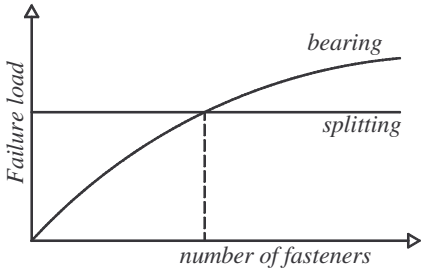

Figure 4: Principle sketch of failure mechanism being dependant on the number of fasteners

2 Experimental program

In order to obtain the intended results described in the previous chapter three series of experiments were conducted: 9 constrained embedding tests (A_i), 3 unconstrained embedding tests (B_i) and 9 bending tests on large scale beams (C_i). Three different fastener diameters were chosen, all with a smooth surface. The figures below show a graphical representation of all specimens. The timber species used was Norway Spruce (*Picea Abies*), with an average density ρ_{12} = 456 kg/m³ and a moisture content ω = 13.0 %. Prior to testing the specimens were stored in a climate room with a temperature of 20±2°C and 65±5 % relative humidity.

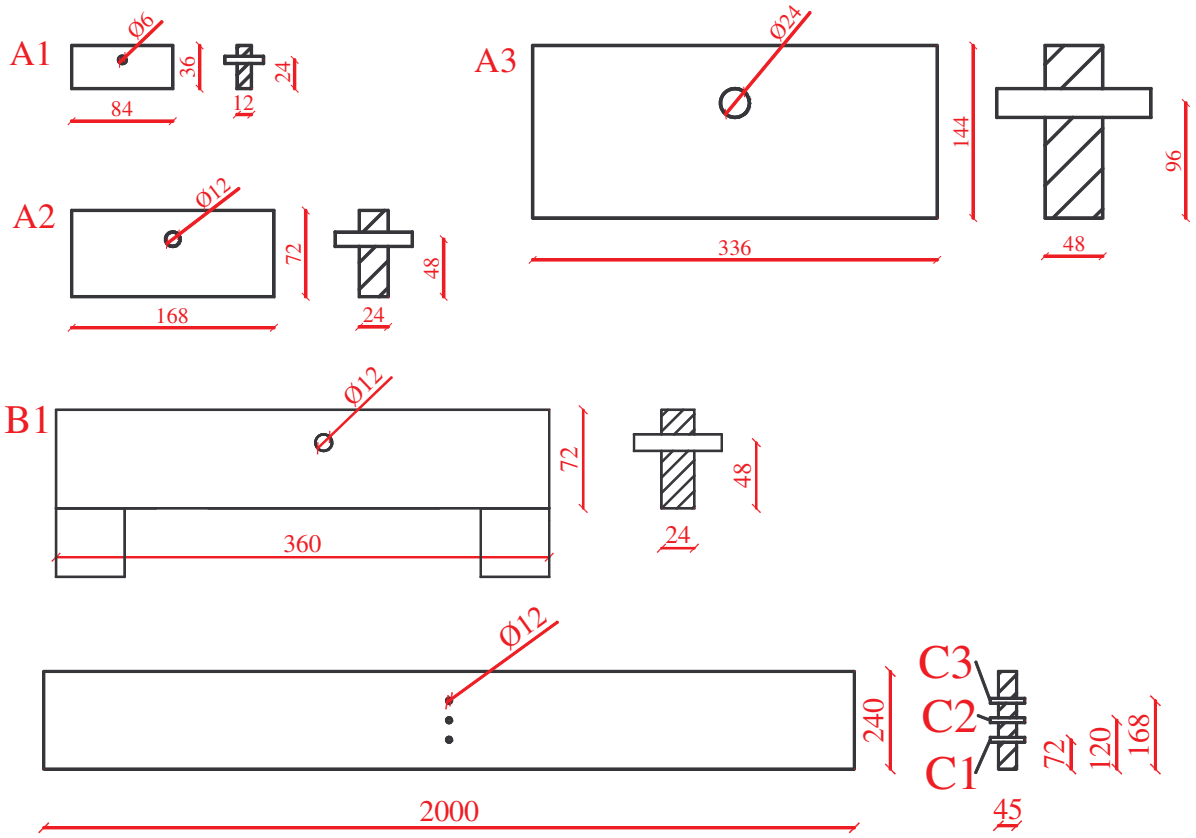

Figure 5: Specimens geometries of three different test series: A: constrained, B: unconstrained, C: bending

The specimen dimensions where set and expressed in relation to the fastener diameter, d. In series A and B the loaded edge distance was set as 4d, the unloaded edge as 2d, the thickness as 2d and the length as 14d (series A). The span in series B_i was fixed as 260 mm, e.g. the supports are 50 mm of length. Within test series C_i the loaded edge distance was varied.

2.1 Experimental set-up and ARAMIS

ARAMIS is a non-contact full-field optical 3D deformation measuring system. The equipment combines digital speckle photogrammetry with 3D correlation techniques and

thereby provides full-field 3D deformation measurements. From these the system calculates and presents 2D strain fields.
The embedment tests of test series A and B were conducted by an Instron 5500R test rig at a constant rate of displacement of 0.5 or 0.8 mm/min. Per series at least two specimens were recorded by ARAMIS during the whole test duration. In the figure below the set up with the ARAMIS equipment is illustrated. Calibration of the measuring volume is carried out according to GOM ARAMIS User Manual [8], i.e. with a cross 300 x 300 mm² with the distance between the cameras fixed at 470 mm, while the measuring length was 1120 mm. In order to obtain bright pictures it is recommended to illuminate the specimens, as is done by means of two cold light sources.

Figure 6: Experimental set-up with ARAMIS

Digital camera images are captured during deformation of the specimen using two cameras. By arranging two cameras at an angle in front of the same specimen area, the displacement captured at the same instants of time can be correlated. This provides stereoscopic information from which displacements out of plane can be calculated. The system is capable of capturing images at a maximum frame rate of 7 Hz.

2.2 Load introduction device

In order to conduct the tests a special load introduction devices had to be manufactured. The use of ARAMIS requires a direct illumination of the specimen surface, and therefore conventional steel side plates can't be used, i.e. the steel side plates have to be modified. These plates need to be rigid and fully clamped (no rotational degrees of freedom) into the test device to stabilize the test. The figure shows a principle sketch.

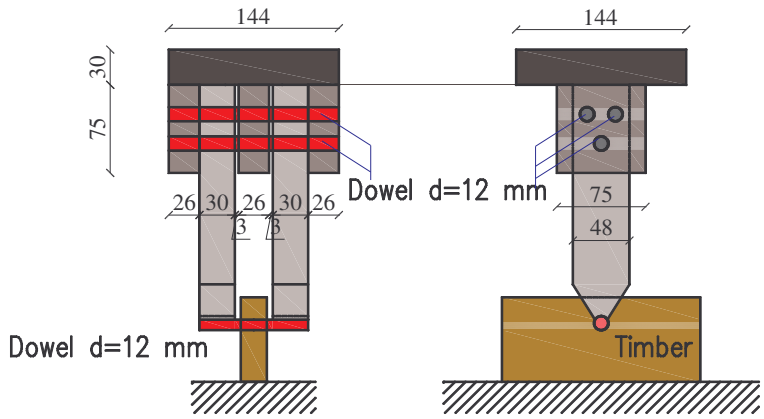

Figure 7: Example of the load introduction principle for embedding test

2.3 Analyses of test series A_i

Test series A consists of the full constrained test specimens. Figure 8 typical load-slip characteristics are depicted. As can be noticed from the figure only a very small amount of deformation is needed to obtain hardening of the load-carrying capacity.

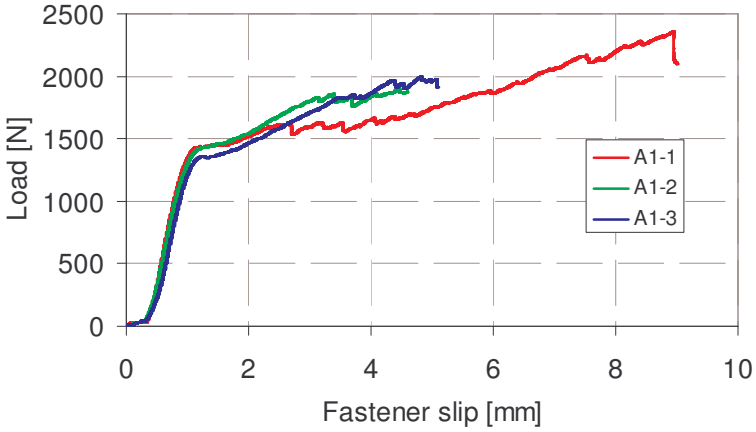

Figure 8: Load-slip response of series A1,i (constrained specimen)

Figure 9 shows the strain perpendicular to the grain on the surface of specimen $A_{1\text{-}1}$, as well as the numerical values at three different sections.

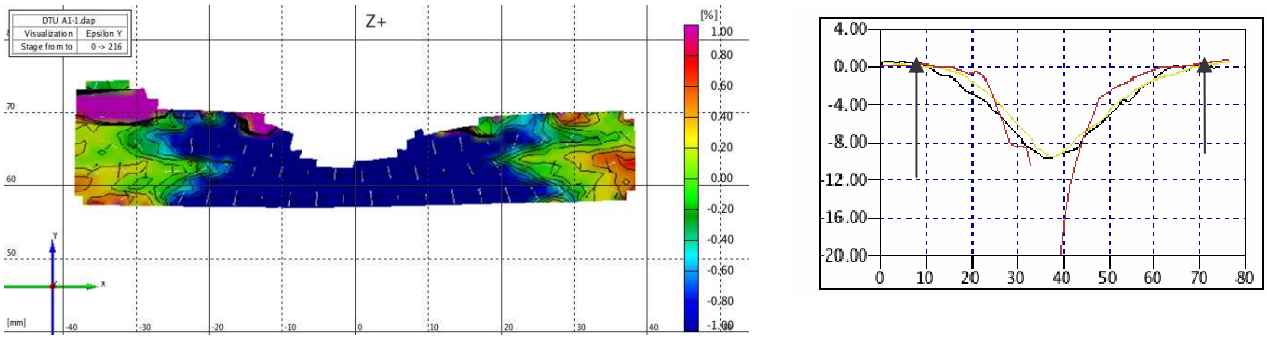

Figure 9: Strain perpendicular to grain in the final stage of specimen $A_{1\text{-}1}$. Arrows mark the intersection points of strains in the lower section and the x-axis

From the chart of Figure 9 it is noticed that indeed spreading of loads (load sharing within the material) does occur. The distance between both intersections between the lower section line and the x-axis (marked by arrows) is approximately 60 mm, see Figure 9. The loaded edge distance in these tests was 4d = 24 mm. From this it follows that the angle of the stress distribution is atan(24/30) ≈ 39°, i.e. 1:1.25.

The strains perpendicular to the grain of another specimen, $A_{2\text{-}1}$, are depicted in Figure 10. The scale is fixed (compression only) in order to obtain a clear image. This specimen shows a triangular strain shape as well if only the large concentrations are regarded (underneath the fasteners), similarly as the previously discussed specimen.

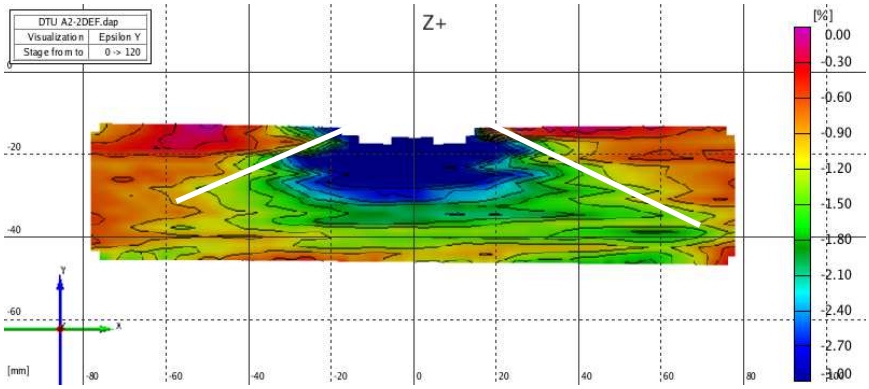

Figure 10: Strain perpendicular to grain in the final stage of specimen A2-2

2.4 Analyses of test series B_i

The specimens of series B are the non-constrained specimens as shown in Figure 2. Because of the dimensions the results can be compared with series A2-i, which is a similar specimen with full constrained boundary conditions over the specimen length. It can be noticed from the load-slip charts, Figure 11, that hardening did occur but didn't develop as much as in the constrained tests of series $A_{2\text{-}1}$.

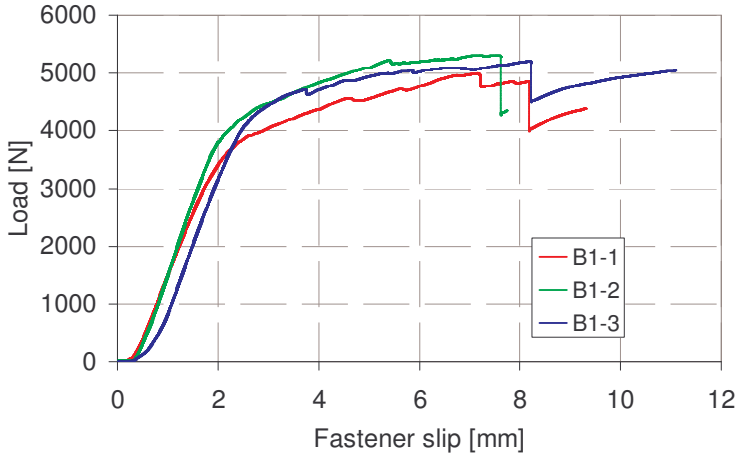

Figure 11: Load-slip response of series B1,i (unconstrained specimen)

In Figure 12 the strains perpendicular to the grain are depicted at several sections at the final stage of loading. The strain shape appears to be more circular than triangular. This was found in test series C_i as well (shown further on). From this it is concluded that the tensile-bending strains in the specimen affects and interacts with the compressive strains originating from the fastener embedment.

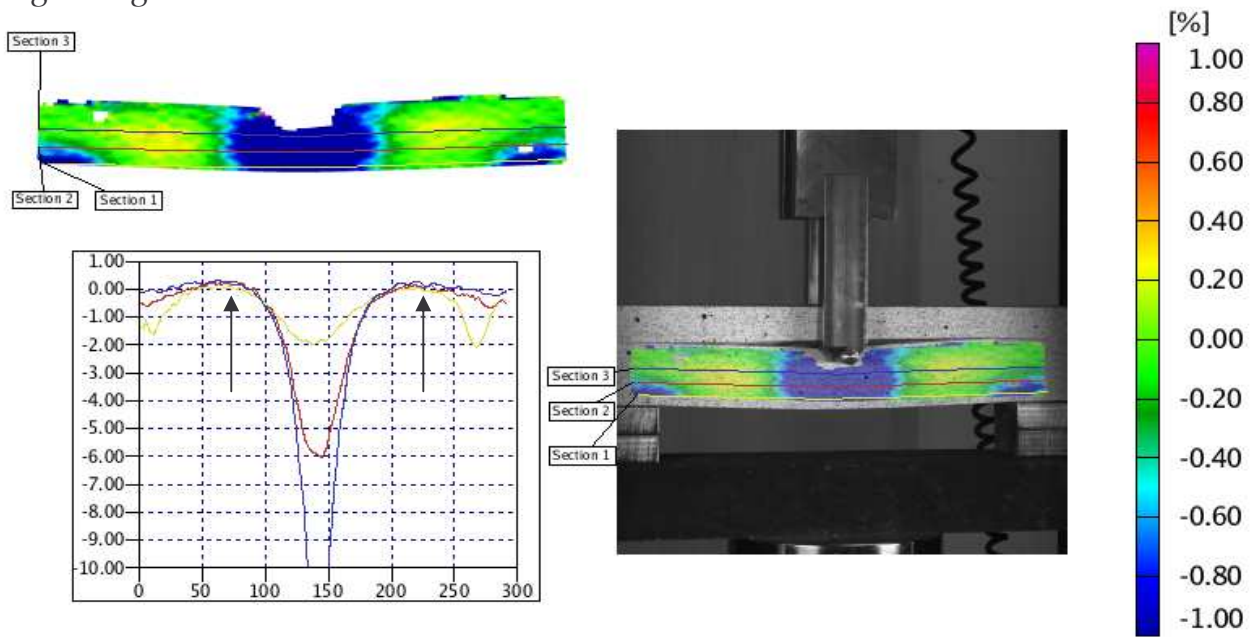

Figure 12: Strain perpendicular to grain in the final stage, specimen B1-3. Arrows mark the intersection points of strains in the lower section and the x-axis

The intersection of lower section line with the x-axis (marked by arrows) now is approximately 140 mm. With a loaded edge distance of 48 mm, an angle of $\theta = \text{atan}(48/70) \approx 34^{\circ}$. This corresponds fairly well with a distribution of 1:1.5, as obtained from tests on timber sills (Van der Put [9]).

2.5 Analyses of test series C_i

In this section the bending tests with one dowel at mid span are analysed. The only parameter varied is the loaded edge distance (h_e) in a way that $\alpha = h_e/h = \{0.3, 0.5, 0.7\}$. Therefore the fastener is located in the tensile and compression zone, as well as in the neutral axis. This feature appears to be of great influence on the load bearing capacity as well as on the appearance of the connection zones after failure. The figures below show subsequently pictures of the fastener holes for $\alpha = \{0.3, 0.5, 0.7\}$, after failure. It can thus be concluded that an increase in loaded edge distance results in an increase in plastic deformation of the timber and thus large hole elongations.

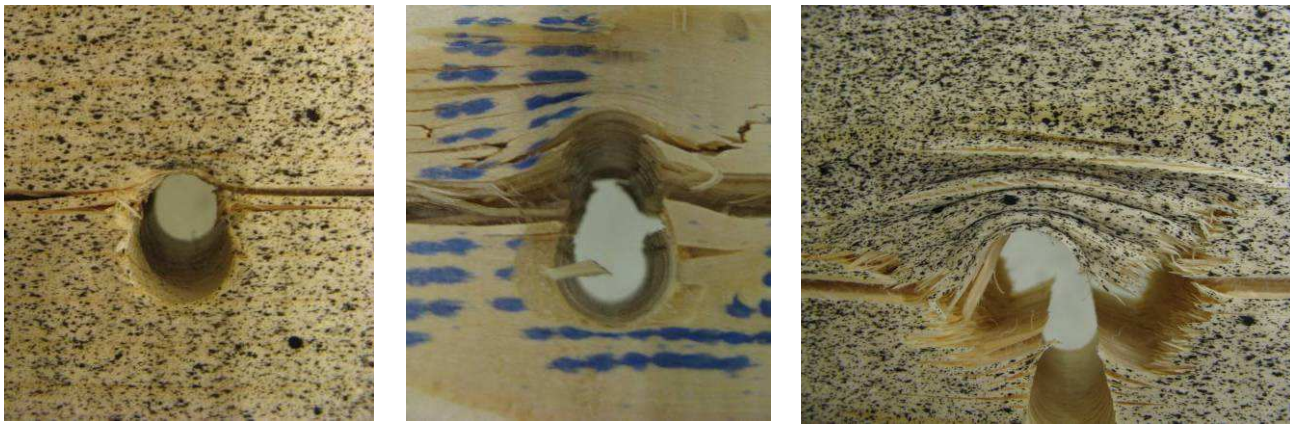

Figure 13: Fastener holes after failure of bending test specimens (series C)

$\alpha = 0.3$ $\alpha = 0.5$ $\alpha = 0.7$

Another feature which appears to be different among test specimens C_i is the shape of the strains. These strains are shown in Figure 14 and 15 for one specimen per series. The scales are fixed (compression only). From these figures a compression zone can be noticed as well, although the angle under which the strains develop is approximately 45° instead of the shallower angle previously found. In the figures below the strain shape is highlighted by means of straight lines. These lines however are questionable and a circular strain shape can be noticed as well. It may therefore be concluded that the shape depends on ones interpretation, and therefore is somewhat ambiguous.

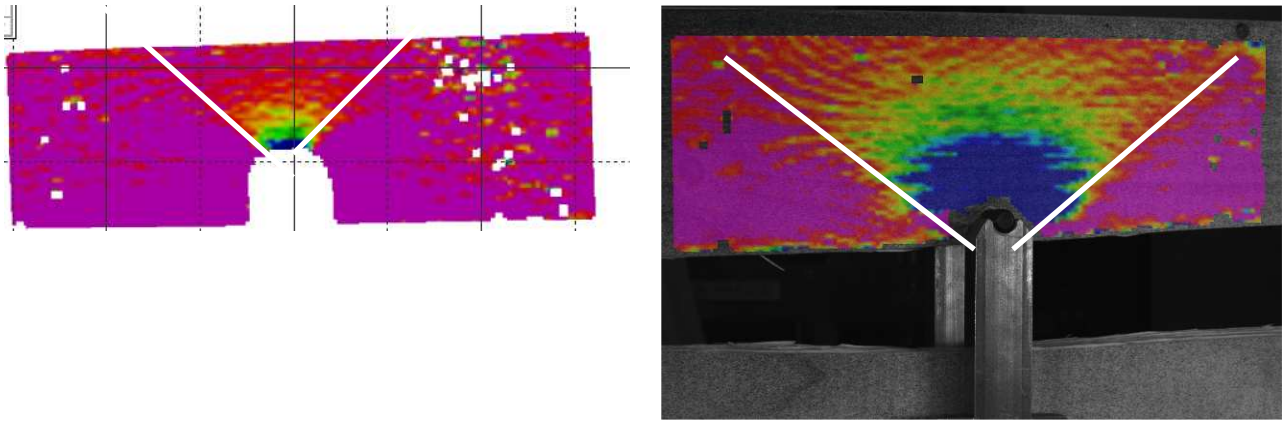

Figure 14: Strains perpendicular to the grain of two bending specimens with two loaded edge distances (αh)

$\alpha = 0.3$ $\alpha = 0.5$

In Figure 15 the perpendicular to grain strains are given for a specimen with $\alpha = 0.7$. This figure shows a clear circular strain shape. Because there is no reason to assume that the strain shape will be influenced by the loaded edge distance, it is concluded that in case of bending stresses in the specimens the shape will change from a triangle to a circle.

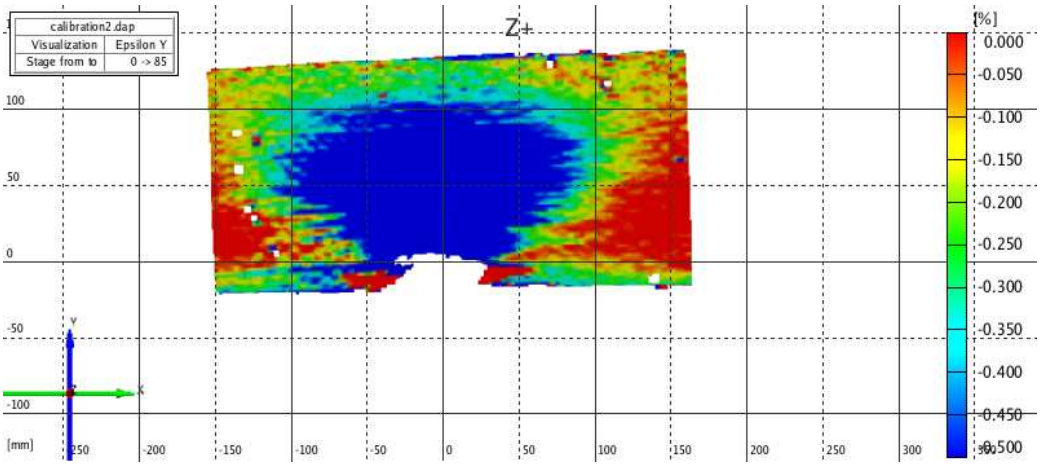

Figure 15: Strains perpendicular to grain of specimen C3-2 with large loaded edge distance (α = 0.7)

2.6 Finite element modeling

In order to verify the shape of the stress distributions some finite element calculations were conducted with the FEM program COMSOL. Figure 16 shows the perpendicular to grain stress distribution of an orthotropic (left) and an isotropic (right) specimen as well as the principle directions of stress. The specimens are full constrained. The stress shape looks very similar as measured by ARAMIS (series Aj-i), although the ARAMIS pictures show strains. The scale is fixed.

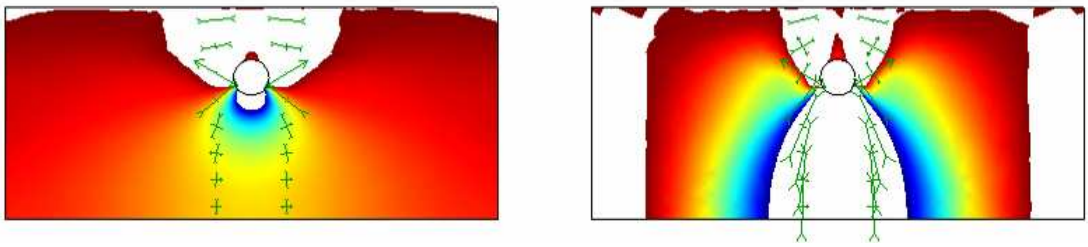

Figure 16: Stress perpendicular to the grain (FEM). Left: Orthotropic material model. Right: Isotropic material model

Figure 17 compares the stresses perpendicular to grain of a constrained embedding test and a bending embedding test, i.e. series A and B. The stress shape seems to be circular in the case of bending. This is confirmed by the ARAMIS measurements. The principle directions of stress are different among both situations as well, notice the direction and size of the arrows.

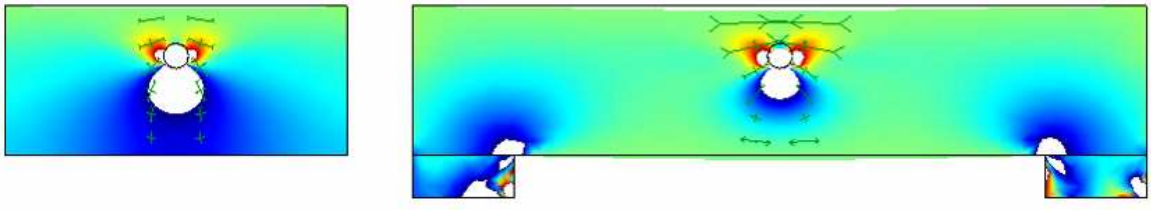

Figure 17: Stress perpendicular to the grain (FEM): Left: constrained test (A2-1). Right: unconstrained test (B1-i)

Since the stress distributions according to the FE-models agree well with the strain distributions measured by ARAMIS, it is assumed that strains and stresses relate through the generalized Hooke's law for orthotropic materials.

Conclusions

This paper describes the research activities carried out during the short term scientific mission by ir. Dennis Schoenmakers under supervision of dr. Staffan Svensson. The main objectives of the research were to determine the angle under which concentrated compression stresses will be distributed through the timber specimen, and to investigate similarities in the embedment (bearing) behaviour underneath a fastener during an embedment tests and during a bending test. In both situations the load was introduced by a fastener. If more knowledge about both aspects is obtained, it will become possible to verify a theoretically based model to describe the bearing strength perpendicular to the grain. Besides, tests in literature with single dowel connections at mid span of a beam can be analysed in more detail, from which it may follow that these specimens didn't fail by primary splitting cracks but that embedding perpendicular to the grain was the main cause of failure and thus the failure mechanism.

For these purposes 21 experiments have been conducted, i.e. 9 constrained embedding tests, 3 unconstrained embedding tests and 9 bending tests. During these experiments the displacement fields are recorded by means of the non-contact full-field optical 3D deformation measuring system ARAMIS (GOM).

The strain distributions underneath the fasteners in the full constrained tests appeared to be triangular shaped what can be expected according to the theory of plasticity. Analyses of the test results of the unconstrained embedding tests shows that under all fasteners a more or less circular stress distribution occurred prior to reaching the ultimate loading level. The angle under which this feature occurs is approximately 1:1.5, as assumed in a theoretically based model. Prior to failure the timber underneath the fastener is highly deformed and crushed which caused the material to yield locally.

Comparison of test series B1,i and A2,i shows that a bending moment in a beam reduces the load spreading through the specimens. Apparently, the bending tensile zone reduced the compression stresses and the triangular shape of the compression stresses has changed into a circular one. This last feature is confirmed by finite element analyses. The tensile-bending zone also leads to limited hardening behaviour what can be noticed from the load-slip diagrams.

Analyses of test series Ci,j shows that the loaded edge distance has great influence on the load bearing capacity, and also on the embedment deformation underneath the fastener. If the loaded edge distance is increased, the deformation increases strongly resulting in very

high local compression stresses and yielding of the timber. Al bending specimens did show crack formation next to the dowel holes, although not prior to yielding of the compressed timber fibres. The compression stress distribution appears to be circular during these tests as well.

Acknowledgement

This paper is a result of a Short Term Scientific Mission in the framework of and supported by COST Action E55, for which the author wishes to acknowledge. The general project is supported by the Dutch Technology Foundation STW, applied science division of NWO and the Technology Program of the Ministry of Economic Affairs, for which the author wishes to acknowledge as well.

References

[1] Comité Européen de Normalisation (CEN): *EN 1995-1-1: 2004: Eurocode 5 - Design of timber structures. Part 1.1: General rules and rules for buildings*. 2004, CEN, Brussels, Belgium.

[2] Sawata, K. and Yasumura, M.: *Determination of embedding strength of wood for dowel-type fasteners*. In: Journal of Wood Science nr 48, 2002, The Japan Wood Research Society, Institute of Wood Technology, Akita, Japan.

[3] Leijten, A.J.M., Köhler, J., and Jorissen, A.J.M.: *Review of probability data for timber connections with dowel-type fasteners*. Proceedings of CIB-W18 / paper 37-7-13, 2004, Edinburgh, Scotland.

[4] Whale, L.R.J. and Smith, I.: *Mechanical Joints in Structural Timberwork - Information for Probabilistic Design*. Timber Research and Development Association, 1986, Buckinghamshire, England.

[5] Comité Européen de Normalisation (CEN): *EN383: Timber Structures. Test methods. Determination of embedding strength and foundation values of dowel type fasteners*. 1993, CEN, Brussels, Belgium.

[6] Van der Put, T.A.C.M. and Leijten, A.J.M.: *Evaluation of perpendicular to grain failure of beams caused by concentrated loads of joints*. Proceedings of CIB-W18 / paper 33-7-7, 2000, Delft, The Netherlands.

[7] Ballerini, M.: *A new set of experimental tests on beams loaded perpendicular-to-grain by dowel-type joints*. Proceedings of CIB-W18 / paper 32-7-2, 1999, Graz, Austria.

[8] GOM Optical Measuring Techniques: *ARAMIS User Manual, ARAMIS 4M v5.4.1*. Gesellschaft für optische Messtechnik (GOM), 2005,

[9] Van der Put, T.A.C.M.: *Derivation of the bearing strength perpendicular to the grain of locally loaded timber blocks*. Publication of Delft Wood Science Foundation, 2006, www.DWSF.nl.